

# Structural and vibrational stability of *M* and *Z* phases of silicon and germanium from first principles

A. Bautista-Hernández,<sup>1,a)</sup> T. Rangel,<sup>2,3</sup> A. H. Romero,<sup>4,5,6,a)</sup> G.-M. Rignanese,<sup>2,3</sup> M. Salazar-Villanueva,<sup>1</sup> and E. Chigo-Anota<sup>7</sup>

<sup>1</sup>Facultad de Ingeniería, Benemérita Universidad Autónoma de Puebla, Apdo. Postal J-39, Puebla, Pue. 72570, Mexico

<sup>2</sup>Institute of Condensed Matter and Nanosciences (IMCN), Université Catholique de Louvain, Chemin des Étoiles 8 bte L7.03.01, B-1348 Louvain-la-Neuve, Belgium

<sup>3</sup>European Theoretical Spectroscopy Facility, ETSF

<sup>4</sup>CINVESTAV, Departamento de Materiales, Unidad Querétaro, Querétaro 76230, Mexico

<sup>5</sup>Max-Planck-Institute für Mikrostrukturphysik, Weinberg 2, D-06120, Halle, Germany

<sup>6</sup>Physics Department, West Virginia University, Morgantown, West Virginia 26506, USA

<sup>7</sup>Facultad de Ingeniería Química, Benemérita Universidad Autónoma de Puebla, Av. San Claudio y 18 Sur S/N Edificio 106A, C.U. San Manuel, 72570 Puebla, Mexico

(Received 11 February 2013; accepted 26 April 2013; published online 15 May 2013)

First-principles calculations were performed to investigate the structural feasibility of *M* and *Z* phases (novel monoclinic and orthorhombic structures recently reported for carbon) for silicon and germanium. The lattice parameters, bulk modulus, vibrational properties, and elastic constants are calculated using the local density approximation to describe the exchange-correlation energy, while the optical properties are calculated by using Many-Body Perturbation Theory in the  $G_0W_0$  approximation. Our results indicate that silicon and germanium with the proposed crystal symmetries are elastically and vibrationally stable and are small band-gap semiconductors. We discuss the possible synthesis of such materials. © 2013 AIP Publishing LLC. [<http://dx.doi.org/10.1063/1.4804668>]

## I. INTRODUCTION

The search of allotropes and polymorphs of single elements and polyatomic compounds has attracted considerable attention from both theoretical and experimental researchers. Indeed, since most of chemical and physical properties depend on the crystal structure, it is expected that materials with new crystal structures might show novel properties. Among the important future electronic components, those based on carbon are very promising. Indeed, its most stable phase is a planar  $sp^2$  structure (graphite) and it has a wide variety of allotropes such as graphene,<sup>1</sup> fullerenes,<sup>2–4</sup> nanotubes,<sup>5,6</sup> and other more complicated structures,<sup>7</sup> leading to a large variety of electronic properties. The carbon family also formed by silicon and germanium has a similar atomic electronic configuration with the same number of valence electrons: they have an open-shell  $p$  orbital with only four electrons, leading to the possibility of finding a diverse set of geometries due to different hybridization as in the case of carbon. Just to cite a few examples, Fujimoto *et al.* recently reported two new silicon and germanium phases with body-centered tetragonal (*bct*) unit cells.<sup>8</sup> Using *ab initio* evolutionary structural search, Li *et al.* have discovered a new carbon phase with a monoclinic structure (referred to as *M* phase) with hardness comparable to diamond.<sup>9</sup> Applying *ab initio* random structure search on the phase diagram of silicon, Malone *et al.* have identified a new phase with the *Ibam* crystal structure.<sup>10</sup> More recently, Amsler *et al.*<sup>11</sup> have found a new orthorhombic form of cold-compressed graphite

(called *Z* phase) showing the *Cmmm* symmetry and composed by  $sp^3$  bonds. All these previous studies have opened the possibility for a broader search of new allotropes of silicon and germanium (in the absence of pressure) possibly showing novel properties within these materials. For instance, Wu *et al.* have investigated the vibrational stability and characterized the electronic properties of two of these new allotropes (*bct* and *M*-phase) of silicon,<sup>12</sup> discussing their possible use as anode materials for lithium batteries.<sup>12</sup> While Malone and Cohen have recently published a quite complete report of different Germanium phases,<sup>13</sup> some considered in this work for reference, neither the *Z* nor the *M* phases were considered in this original work. On the other hand, recently there has been strong interest in the *Z* phase of carbon, where the elastic constants, stress-strain diagram, vibrational stability, hardness, and Raman spectrum were detailed studied. From these results, it has been shown that the carbon *Z* has hardness comparable to diamond.<sup>14,15</sup>

On the other hand, various silicon and germanium allotropes such as cubic diamond, *allo*<sup>16–18</sup> clathrate,<sup>19,20</sup> and nanotube phases<sup>21,22</sup> have been synthesized at ambient pressure. Some other allotropes can be synthesized under hydrostatic conditions, such as  $\beta$ -Sn, *Imma*, simple hexagonal, *Cmca*, and hexagonal close packed phases. Even more complex phases can be obtained by decompression of the  $\beta$ -Sn phase (such as R8, BC8, and ST12). This large number of allotropes has motivated the theoretical study of new phases of silicon and germanium. From the pioneering work of Joannopoulos and Cohen,<sup>23,24</sup> who performed predictions of new allotropes of silicon and germanium with different physical properties of the diamond phase, a long path has been committed into new crystal structures based on these atoms. We refer the reader to

<sup>a)</sup>Authors to whom correspondence should be addressed. Electronic addresses: [alejandro.bautista@correo.buap.mx](mailto:alejandro.bautista@correo.buap.mx) and [aromero@qro.cinvestav.mx](mailto:aromero@qro.cinvestav.mx)

some of the published papers to find details of the many different considered structures, in particular those by Needs *et al.*,<sup>25</sup> Pfrommer *et al.*,<sup>26</sup> Malone *et al.*,<sup>10,13,27–29</sup> and more recently by Zhao *et al.*<sup>30</sup> and Zhai *et al.*<sup>31</sup>

In the present work, we report on a first-principles study of silicon and germanium in the *M* (space group *C2/m*, monoclinic) and *Z* (space group *Cmmm*, orthorhombic) phases, as reported in Refs. 9 and 11. These are compared with the lowest energy structure for Si and Ge, the diamond structure (space group *Fd3m*, cubic). We perform a structural, vibrational and elastic stability study as well as an optical characterization. Section II describes the theoretical methods used to perform the different characterizations while Sec. III discusses the results obtained for the considered monoclinic and diamond unit cells. Finally, we present some conclusions and perspectives in the last section.

## II. CALCULATION METHODS

The structural parameters of the diamond, *M* and *Z* phases of silicon and germanium are optimized using Density Functional Theory.<sup>32</sup> The exchange-correlation energy is described through the Local Density Approximation (LDA), as parametrized by Perdew and Zunger.<sup>33</sup> In order to study the influence of the chosen exchange-correlation functional, we also calculate the structural and elastic properties using the Generalized Gradients Approximation (GGA) functional proposed by Perdew, Burke, and Enzerhof.<sup>34</sup> Since the obtained errors (with respect to experimental data) in the elastic constants are larger than those obtained with the LDA functional for the diamond phase,<sup>34</sup> we restrict ourselves by using LDA for the rest of properties. We use the Hartwigsen-Goedecker-Hutter (HGH) relativistic separable dual-space Gaussian pseudopotential<sup>35</sup> within the ABINIT code and Vanderbilt ultrasoft pseudopotential<sup>36</sup> for the CASTEP code to describe the valence electrons. The Kohn-Sham orbitals and electron density are expanded in terms of a plane-wave basis set with an energy cut-off of 700 and 750 eV for Si and Ge, respectively. The Brillouin zones are sampled using  $10 \times 10 \times 10$ ,  $10 \times 10 \times 8$ , and  $8 \times 8 \times 16$  Monkhorst-Pack<sup>37</sup> grid k-points for the diamond, *M* and *Z* phases, respectively. Special attention is paid to the relaxation of the internal degrees of freedom of the monoclinic and orthorhombic structure, which have eight atoms per unit cell. The bulk modulus is obtained by fitting the total energy versus volume with a third order Birch-Murnaghan (BM) equation of state.<sup>38</sup>

We calculate the elastic constants by means of two different methods, as well as two different pseudopotentials. Basically, we use the finite strain method<sup>39</sup> and Density-Functional Perturbation Theory (DFPT)<sup>40</sup> as implemented in the CASTEP<sup>41</sup> and ABINIT<sup>42</sup> codes, respectively. The phonon dispersion relations are obtained within the linear response theory as implemented in the ABINIT code.<sup>42,43</sup> The dynamical matrices are computed on a  $6 \times 6 \times 7$  mesh of q-points, and then a Fourier interpolation is employed to obtain the phonon frequencies in the full Brillouin zone.

The band-structures and optical properties are calculated using Many-Body Perturbation Theory (MBPT) within the one-shot  $G_0W_0$  approximation<sup>44</sup> as implemented in the

ABINIT code. An  $8 \times 8 \times 9$  Monkhorst-Pack grid of k-points is used for both silicon and germanium in the *M* and *Z* phases. For the materials in the diamond phase, a denser mesh with 328 k-points is used. It is defined as the reciprocal lattice of a supercell lattice defined by the three vectors: (11,−11,0), (11,0,11), and (0,−11,11). Trouiller-Martins pseudopotentials are used for the  $G_0W_0$  and optical response calculations (HGH pseudopotentials cannot be used for  $G_0W_0$  calculations in ABINIT). The dielectric matrix is calculated using the Adler-Wiser expression summing over 64 bands. Local-field effects are taken into account adopting an energy cut-off of 136 eV, corresponding to a matrix size of 181, 585, and 573 (resp. 169, 649, and 641) plane waves for the diamond, *M* and *Z* phases of Si (resp. Ge). To accelerate the convergence with respect to the number of bands treated explicitly, we use the extrapolar method described in Ref. 45. The  $G_0W_0$  corrections are calculated for 36 bands and 328, 165, and 189 irreducible k-points corresponding to the k-grids mentioned above for the diamond, *M* and *Z* phases, respectively. The band-structures are then obtained using an interpolation scheme based on maximally localized Wannier functions, as explained in Refs. 46 and 47.

In the case of the optical calculations, we use norm-conserving pseudopotentials without semi-core states, since it was found that including them worsens the agreement with experiments, for Si and Ge diamond.<sup>48,49</sup> The optical properties are obtained with the DP code<sup>50</sup> and compare with the ABINIT results using 30 bands in the calculation of the dielectric functions. Local-field effect are accounted for taking a matrix size of 51 plane waves, corresponding to an energy cutoff of 54, 27, and 25 eV (resp. 52, 22, and 23 eV) for the diamond, *M* and *Z* phases of Si (resp. Ge). The optical properties are calculated using the same k-point mesh as for the  $G_0W_0$  calculations. Moreover, a Gaussian broadening of 0.12 eV is used. To account for excitonic effects, time-dependent DFT (TDDFT) is used adopting the long-range kernel derived in Ref. 51, with the parameter  $\alpha = 0.2$ . This approximation yields excellent agreement between the calculated and the experimental absorption spectrum of silicon bulk in the diamond phase.

The above mentioned computation parameters (energy cutoffs, k-point and q-point grids, number of bands) guarantee errors smaller than 1 meV/atom on the total energy, 0.1 GPa on the elastic constants,  $3 \text{ cm}^{-1}$  on the phonon frequencies,  $\sim 1 \text{ meV}$  on the QP energies, and a convergence in the optical spectra up to 10 eV.

## III. RESULTS AND DISCUSSIONS

In order to check the validity of the pseudopotentials, we compare the calculated elastic constants based on the parameters described in Sec. II with the experimental results reported in Ref. 52 for the Si and Ge diamond phases. From our results, we observe a closer agreement with the HGH pseudopotentials.<sup>53</sup> Therefore, for the *M* and *Z* phases, we only used the HGH pseudopotentials to describe the core electrons. Table I shows the cell parameters, bulk modulus, shear modulus (*G*), and Young modulus (*E*). The bulk modulus obtained from the BM equation is in parentheses. We can

TABLE I. Cell parameters and bulk modulus for silicon and germanium in the diamond, *M* and *Z* phases.

Element	a (Å)	b (Å)	c (Å)	$\beta$ (degrees)	B (GPa)	G (GPa)	E (GPa)
<b>Si</b>							
Diamond (this work)	5.40	...	...	...	95.9 (94.1)	82.8	126.5
Diamond (Exp. Refs. 54 and 55)	5.43	...	...	...	102	...	...
<i>M</i> -Si (this work)	13.67	3.80	6.28	96.73	87.9 (89.6)	71.7	192.5
<i>M</i> -Si (Ref. 11)	13.90	3.863	6.359	...	...	...	...
<i>Z</i> -Si (this work)	7.33	7.33	3.79	...	91.6	68.0	146.6
<b>Ge</b>							
Diamond (this work)	5.58	...	...	...	72.9 (72.4)	68.5	103.0
Diamond (Exp. Refs. 54 and 55)	5.66	...	...	...	77	...	...
<i>M</i> -Ge (this work)	14.18	3.95	6.49	96.79	67.2 (68.0)	59.7	174.8
<i>Z</i> -Ge (this work)	7.60	7.60	3.94	...	69.8	56.6	119.9

see that in the case of the lattice parameters for silicon and germanium in the diamond phase, there is good agreement with available experimental data,<sup>54,55</sup> with maximum errors of 1%. In the case of the bulk modulus and the elastic constants, we obtain very similar values to those calculated from the BM equation, with maximum differences of 2 GPa. The maximum errors with respect to experimental data are 5.9%. These error percentages are typical of first principles calculations. Table I also shows the lattice parameters, the  $\beta$  angle, bulk modulus, shear modulus, and Young modulus of the monoclinic and orthorhombic structures for silicon and germanium. For the *M* phase, the  $\beta$  angle values for silicon and germanium are very similar to those for carbon.<sup>9</sup> In the case of the *M* phase of silicon, the lattice parameters obtained in this work are in agreement with those reported by Wu *et al.*<sup>12</sup> The calculated mechanical moduli (B, G, E) provide us with an idea of the mechanical behavior of the studied materials. The bulk modulus is the resistance to hydrostatic compression, while the shear and Young moduli describe the mechanical behavior under shear and uniaxial deformation. In general, the bulk moduli in the *M* phases are slightly smaller than in the diamond phase, which means a smaller compressibility for these phases. The same behavior is obtained for the shear modulus, whose values are smaller than the diamond phase. On the other hand, the Young's moduli for the monoclinic phases are larger than in the diamond phase. While in the case of the *Z* phase of silicon, the modules of compressibility and Young's are larger than in the diamond phase. In both cases, this means a greater mechanical resistance to compression and uniaxial deformation. Along the same line, the Germanium *Z* phase shows better mechanical resistance to uniaxial deformation.

In order to evaluate the thermodynamic stability of the different phases, it is common to perform total-energy calculations over all experimentally observed phases as well as for various predicted metastable phases (see, e.g., Ref. 10). Here, we focus on those that are the most stable ones in the absence of pressure. Hence, in addition to the diamond, *M* and *Z* phases, we also consider the *bct* phase, which is metastable at hydrostatic tensile pressures,<sup>8</sup> as it is the case of *M* and *Z* phases for silicon and germanium. Figure 1 shows the total energy as a function of the volume for silicon and germanium in the different phases. Black squares, red [gray]

circles, green [medium gray] triangles, and yellow [light gray] diamonds indicate the obtained data for diamond, *Z*, *bct*, and *M* phases, respectively, where the lines come from a fitting obtained through the BM equation of state.

The energy of the *M* and *Z* phases with respect to the diamond phase for silicon (0.1 eV/atom and 0.065 eV/atom) and germanium (0.09 eV/atom and 0.062 eV/atom) is similar to the thermal energy ( $k_B T \sim 0.1$  eV), from which we infer that these phases may exist at room temperature or can be synthesized under metastable conditions if the system is properly quenched.<sup>8</sup> The volumes of the *M* and *Z* phases are

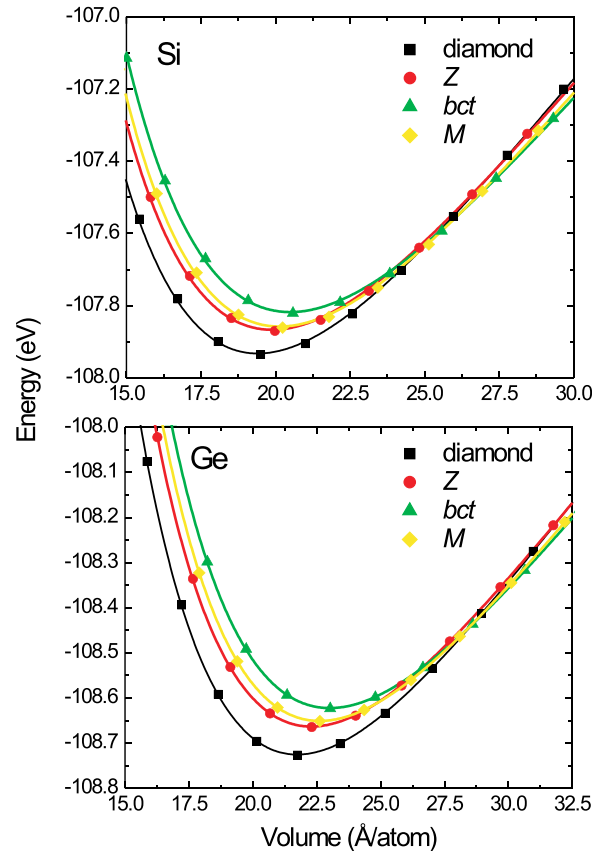


FIG. 1. Total energy curves for silicon and germanium in the diamond, *Z*, *bct*, and *M* phases. The symbols correspond to the calculated data, and the lines are fits to the BM equation of state.

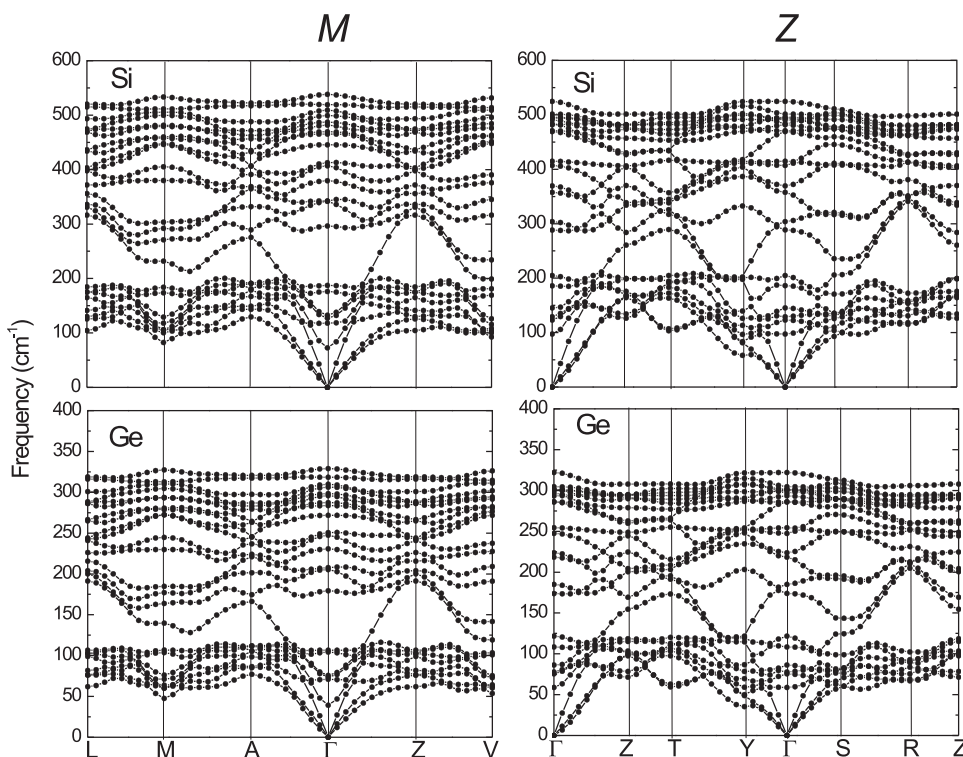
TABLE II. Elastic constants for silicon and germanium in the diamond,  $M$  and  $Z$  phases.

Material/elastic constants	Diamond Si (this work)	Diamond Si (Exp.) Ref. 48	$M$ -Si (this work)	$Z$ -Si (this work)	Diamond Ge (this work)	Diamond Ge (Exp.) Ref. 48	$M$ -Ge (this work)	$Z$ -Ge (this work)
$C_{11}$	161.9	165.78	148.9	169.9	127.3	128.53	124.3	135.3
$C_{22}$			174.7	176.5			140.8	141.6
$C_{33}$			169.8	191.1			136.0	151.9
$C_{44}$	77.1	79.62	69.4	50.7	66.9	66.80	60.5	44.0
$C_{55}$			60.6	60.1			52.3	50.4
$C_{66}$			39.0	36.1			33.6	36.3
$C_{12}$	63.0	63.94	36.9	50.1	45.8	48.26	23.1	35.9
$C_{13}$			59.4	52.4			40.4	37.0
$C_{15}$			12.8				10.9	
$C_{23}$			52.7	40.9			38.2	27.1
$C_{25}$			-6.7				-6.4	
$C_{35}$			7.2				6.8	
$C_{46}$			-2.6				-1.5	

larger than the diamond phase; therefore, these phases could be obtained under tensile stresses.<sup>8</sup>

Table II shows the elastic constants of the diamond,  $M$  and  $Z$  phases for silicon and germanium, calculated by DFPT with HGH pseudopotentials. In the case of the diamond phase, there are three independent elastic constants ( $C_{11}$ ,  $C_{12}$ , and  $C_{44}$ ). For the  $M$ -phase, there are thirteen independent elastic constants ( $C_{11}$ ,  $C_{22}$ ,  $C_{33}$ ,  $C_{44}$ ,  $C_{55}$ ,  $C_{66}$ ,  $C_{12}$ ,  $C_{13}$ ,  $C_{15}$ ,  $C_{23}$ ,  $C_{25}$ ,  $C_{35}$ ,  $C_{46}$ ); and for  $Z$ -phase, there are nine independent elastic constants ( $C_{11}$ ,  $C_{22}$ ,  $C_{33}$ ,  $C_{44}$ ,  $C_{55}$ ,  $C_{66}$ ,  $C_{12}$ ,  $C_{13}$ ,  $C_{23}$ ). The bulk, shear, and Young's moduli were obtained using the Voigt scheme from the values of the elastic constants.<sup>56</sup> Very good agreement is observed between the calculated elastic constants and the experimental data for the diamond phase. Table II also shows the calculated elastic constants for the  $M$  and  $Z$  phases. These values are consistent with the Born-

Huang elastic stability criteria,<sup>57</sup> and therefore both phases are *elastically stable*. On the other hand, to confirm the dynamical stability of silicon and germanium in the  $M$  and  $Z$  phases, we compute their phonon dispersion curves (Fig. 2). The frequencies remain positive throughout the whole Brillouin zone, indicating that Si and Ge are *dynamically stable*. The phonon range is similar to the diamond phase, which goes a bit beyond  $500\text{ cm}^{-1}$  for Si and  $320\text{ cm}^{-1}$  for Ge. The change in the symmetry is clearly visible in the acoustic branches, and no phonon gaps are observed. While in the diamond case, there are two degenerate branches and another branch with larger dispersion, the three acoustic branches are all degenerated and the dispersion is smaller in the  $M$  phases. Notice the similarities in the dispersion relation in the  $M$  phase between the two compounds, which is related to the fact that phonons scale as the inverse of the square root of the ion mass.

FIG. 2. Phonon dispersion relations for silicon and germanium at the  $M$  and  $Z$  phases.

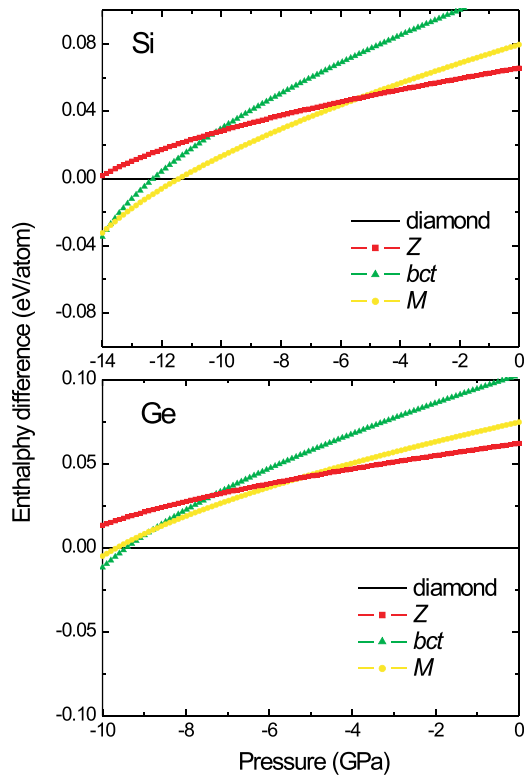


FIG. 3. Enthalpy pressure curves for different phases of silicon and germanium. Black lines, red [gray] squares, green [medium gray] triangles, and yellow [light gray] triangles correspond to diamond, Z, and *M* phases, respectively.

On the other hand, Fig. 3 shows the curves of pressure vs. enthalpy difference for the phases considered in this study. As we can see, there are some possible phase transitions within the considered structures as a function of hydrostatic tensile pressure

diamond  $\rightarrow$  *M* (11.3 GPa)  $\rightarrow$  *bct* (12.3 GPa)  $\rightarrow$  Z (14.1 GPa) for silicon, and  
diamond  $\rightarrow$  *bct* (9.4 GPa)  $\rightarrow$  *M* (9.6 GPa)  $\rightarrow$  Z (11 GPa) for germanium.

The band-structures are calculated using MBPT within the  $G_0W_0$  approximation, which is known to be very accurate in describing the electronic structure of the diamond phases for these systems. For instance, our  $G_0W_0$  gap of diamond Si (Ge) is 1.17 (0.65) eV, in good agreement with the experimental gap of 1.17 (0.74) eV.<sup>58</sup> Therefore, our results for the gaps of the solids in diamond phase are in good agreement with previous works.<sup>49</sup> The band-structures for silicon and germanium in the *M* and Z phases are shown in Fig. 4. The DFT (red [gray] lines) and  $G_0W_0$  (solid lines) results are shown. For *M*-Si, the  $G_0W_0$  indirect gap is of 0.85 eV between the  $\Gamma$  and *M* (0.5, 0.5, 0.5) points. Silicon in the Z phase has a gap of 1.12 eV between the  $\Gamma$  and Y (−0.5, 0.5, 0.0) points. For *M*-Ge, the  $G_0W_0$  gap is of 0.30 eV. Here, the top of the valence band (TVB) is at  $\Gamma$ , whereas the bottom of the conduction band (BCB) is located between  $\Gamma$  and *M* (at  $\sim 57\%$  of their distance) in the Brillouin zone. The Z-Ge structure has a  $G_0W_0$  gap of 0.64 eV. The TVB is at Y and the BCB is at the  $\Gamma$  point. The  $G_0W_0$  corrections, in both materials, corresponds to an almost shift of the electronic bands, as a simple scissors-operator, which happen to be similar to the corrections for the diamond structures of silicon and germanium.

Figure 5 shows the imaginary part of the dielectric function of silicon and germanium in the diamond (solid lines), *M* (green [medium gray] lines and square symbols), and Z (red [gray] lines and circle symbols). In the case of silicon, the diamond spectra have two main peaks: an excitonic peak at  $\sim 3.6$  eV and a second peak at 4.4 eV. The *M* phase shows

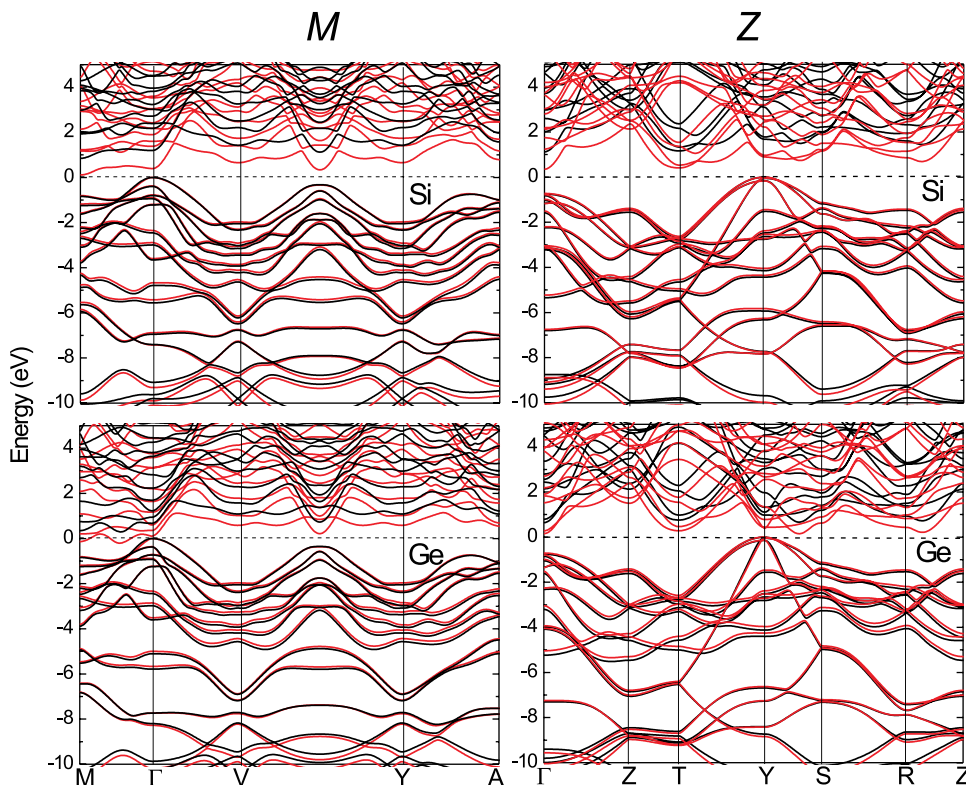


FIG. 4. Energy band structure along high-symmetry lines of the Brillouin zone for silicon and germanium in the *M* and Z phases. Red lines correspond to DFT, while solid lines correspond to the  $G_0W_0$  calculation.

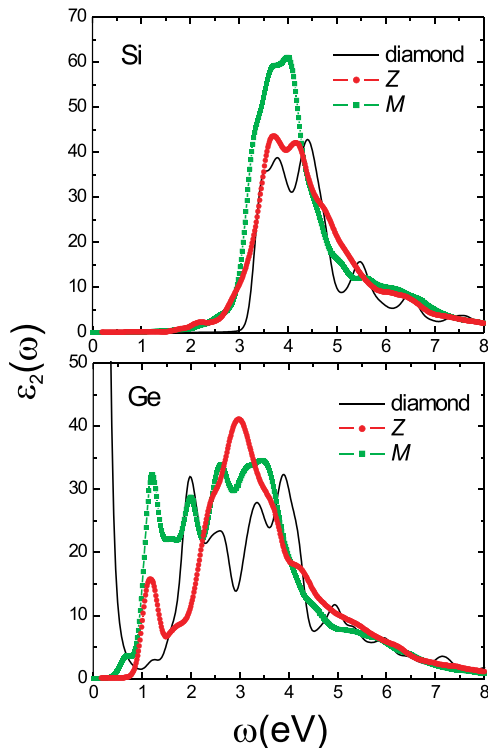


FIG. 5. Frequency dependence of the imaginary part of the dielectric function for silicon and germanium in the diamond (black line), *M* (green [medium gray] line and square symbols), and *Z* (red [gray] line and circle symbols) phases.

one main peak centered at  $\sim 3.8$  eV; whereas for the *Z* phase, there are two adsorption maxima at 3.7 and  $\sim 4.1$  eV. Moreover, the spectra of the both the *M* and *Z* phases have a narrower optical adsorption gap, which can directly be linked to the narrower electronic energy band gap. In the case of germanium, the spectrum of the diamond structure has a big excitonic peak at low energies ( $\omega < 0.4$  eV), which is not present in the *M* and *Z* phases. The spectrum of the diamond structure also has several adsorption peaks at  $\sim 2$ , 2.5, 3.3, and 3.0 eV. In the *M* phase spectrum, there are only three main peaks at  $\sim 1.18$ , 2.0, and 2.6–3.0 eV. For *Z* phase, the adsorption spectra consists of a main peak at  $\sim 3.0$  eV and a small shoulder at 1.2 eV.

#### IV. CONCLUSIONS

We have conducted a stability study of silicon and germanium in the *M* and *Z* phases, which have been compared to the diamond phase. From the Born-Huang stability criteria, both the *M* and *Z* phases happen to be elastically and vibrationally stable, with small energy differences with respect to the diamond phase, indicating that these structures can be synthesized at room temperature. Due to the volume differences of these phases with respect to the diamond structure, it may be possible to obtain them from a tensile stress. These phases have a better uniaxial mechanical strength than diamond phases based on the values of Young's modulus. However, in the case of shear deformations and hydrostatic compressibility, the mechanical strength is lower. The optical properties have also been reported and we have found energy bands much smaller than

in the diamond phases. These phases have a different optical behavior, with a reduction of the electronic gap as well as excitonic effects, which happen at smaller energies.

#### ACKNOWLEDGMENTS

This work has been supported by VIEP-BUAP (Grant BAHA-ING13-G) Mexico. The authors would like to acknowledge the National Supercomputer Center (CNS) of IPICYT, A. C. for supercomputer facilities. We (A. H. R., T.R., and G.M.R.) acknowledge support from CONACYT-México under projects 152153 and FNRS-CONACYT México. A.H.R. recognizes the support from the Marie-Curie Intra-European Fellowship.

- <sup>1</sup>K. S. Novoselov, A. K. Geim, S. V. Morozov, D. Jiang, S. V. Dubonos, I. V. Girgorieva, and A. A. Firsov, *Science* **306**, 666 (2004).
- <sup>2</sup>H. W. Kroto, J. R. Heath, S. G. O'Brien, R. F. Curl, and R. E. Smalley, *Nature* **318**, 162 (1985).
- <sup>3</sup>W. Krätschmer, L. D. Lamb, K. Fostiropoulos, and D. R. Hoffman, *Nature* **347**, 354 (1990).
- <sup>4</sup>S. Saito and A. Oshiyama, *Phys. Rev. Lett.* **66**, 2637 (1991).
- <sup>5</sup>S. Iijima, *Nature* **354**, 56 (1991).
- <sup>6</sup>N. Hamada, S. I. Sawada, and A. Oshiyama, *Phys. Rev. Lett.* **68**, 1579 (1992).
- <sup>7</sup>L. R. Radovic and B. Bockrath, *J. Am. Chem. Soc.* **127**, 5917 (2005).
- <sup>8</sup>Y. Fujimoto, T. Koretsune, S. Saito, T. Miyake, and A. Oshiyama, *New J. Phys.* **10**, 083001 (2008).
- <sup>9</sup>Q. Li, Y. Ma, A. R. Oganov, H. Wang, H. Wang, Y. Xu, T. Cui, H.-K. Mao, and G. Zou, *Phys. Rev. Lett.* **102**, 175506 (2009).
- <sup>10</sup>B. D. Malone and M. L. Cohen, *Phys. Rev. B* **85**, 024116 (2012).
- <sup>11</sup>M. Amsler, J. A. Flores-Livas, L. Lehtovaara, F. Balima, S. A. Ghasemi, D. Machon, S. Pailhes, A. Willand, D. Caliste, S. Botti, A. San Miguel, S. Goedecker, and M. A. L. Marques, *Phys. Rev. Lett.* **108**, 065501 (2012).
- <sup>12</sup>F. Wu, D. Jun, E. Kan, and Z. Li, *Solid State Commun.* **151**, 1228 (2011).
- <sup>13</sup>B. D. Malone and M. L. Cohen, *Phys. Rev. B* **86**, 054101 (2012).
- <sup>14</sup>J. Qin, Z. Hou, and X. Zhang, *AIP Adv.* **2**, 022160 (2012).
- <sup>15</sup>Z. Li, F. Gao, and Z. Xu, *Phys. Rev. B* **85**, 144115 (2012).
- <sup>16</sup>H. G. Von Schnering, M. Schwarz, and R. Nesper, *J. Less-Common Met.* **137**, 297 (1988).
- <sup>17</sup>A. Gruttner, R. Nesper, and H. G. Von Schnering, *Angew. Chem., Int. Ed. Engl.* **21**, 912 (1982).
- <sup>18</sup>F. Kiefer, A. J. Karttunen, M. Dobliger, and T. F. Fassler, *Chem. Mater.* **23**, 4578 (2011).
- <sup>19</sup>J. Gryko, P. F. McMillan, R. F. Marzke, G. K. Ramachandran, D. Patton, S. K. Deb, and O. F. Sankey, *Phys. Rev. B* **62**, R7707 (2000).
- <sup>20</sup>A. M. Guloy, R. Ramlau, Z. Tang, W. Schnelle, M. Baitinger, and Y. Grin, *Nature* **443**, 320 (2006).
- <sup>21</sup>Y. H. Tang, L. Z. Pei, Y. W. Chen, and C. Guo, *Phys. Rev. Lett.* **95**, 116102 (2005).
- <sup>22</sup>M.-H. Park, Y. H. Cho, K. Kim, J. Kim, M. Liu, and J. Cho, *Angew. Chem., Int. Edn Engl.* **50**, 9647 (2011).
- <sup>23</sup>J. D. Joannopoulos and M. L. Cohen, *Solid State Commun.* **11**, 549 (1972).
- <sup>24</sup>J. D. Joannopoulos and M. L. Cohen, *Phys. Lett. A* **41**, 71 (1972).
- <sup>25</sup>R. J. Needs and A. Mujica, *Phys. Rev. B* **51**, 9652 (1994).
- <sup>26</sup>B. G. Pfrommer, M. Coté, S. G. Louie, and M. L. Cohen, *Phys. Rev. B* **56**, 6662 (1997).
- <sup>27</sup>B. D. Malone, J. D. Sau, and M. L. Cohen, *Phys. Rev. B* **78**, 161202(R) (2008).
- <sup>28</sup>B. D. Malone, J. D. Sau, and M. L. Cohen, *Phys. Rev. B* **78**, 035210 (2008).
- <sup>29</sup>B. D. Malone, S. G. Louie, and M. L. Cohen, *Phys. Rev. B* **81**, 115201 (2010).
- <sup>30</sup>Z. Zhao, F. Tian, X. Dong, Q. Li, Q. Wang, H. Wang, X. Zhong, B. Xu, D. Yu, J. He, H.-T. Wang, Y. Ma, and Y. Tian, *J. Am. Chem. Soc.* **134**, 12362 (2012).
- <sup>31</sup>J. Zhai, D. Yu, K. Luo, Q. Wang, Z. Zhao, J. He, and Y. Tian, *J. Phys.: Condens. Matter* **24**, 405803 (2012).

- <sup>32</sup>P. Hohenberg and W. Kohn, *Phys. Rev.* **136**, B864 (1964); W. Kohn and L. Sham, *Phys. Rev.* **140**, A1133 (1965).
- <sup>33</sup>J. P. Perdew and A. Zunger, *Phys. Rev. B* **23**, 5048 (1981).
- <sup>34</sup>For this calculation, we use the Generalized Gradient Approximation parameterized by Perdew, Burke and Ernzerhof (J. P. Perdew, K. Burke, and M. Ernzerhof, *Phys. Rev. Lett.* **77**, 3865 (1996)) and Hartwigsen-Goedecke-Hutter pseudopotentials. The results for silicon are:  $C_{11} = 152.9$  GPa,  $C_{12} = 56$  GPa, and  $C_{44} = 74.9$  GPa. For germanium, the results are:  $C_{11} = 103.6$  GPa,  $C_{12} = 35.8$  GPa, and  $C_{44} = 55.4$  GPa. The average errors for the three elastic constants of the two elements are 14.68% and 2.19% for the GGA and LDA functionals, respectively.
- <sup>35</sup>C. Hartwigsen, S. Goedecker, and J. Hutter, *Phys. Rev. B* **58**, 3641 (1998).
- <sup>36</sup>D. Vanderbilt, *Phys. Rev. B* **41**, 7892 (1990).
- <sup>37</sup>H. J. Monkhorst and J. D. Pack, *Phys. Rev. B* **8**, 5747 (1973).
- <sup>38</sup>F. Birch, *Phys. Rev.* **71**, 809 (1947).
- <sup>39</sup>S. Q. Wang and H. Q. Ye, *Phys. Status Solidi B* **240**, 45 (2003).
- <sup>40</sup>D. R. Hamann, X. Wu, K. M. Rabe, and D. Vanderbilt, *Phys. Rev. B* **71**, 035117 (2005).
- <sup>41</sup>S. J. Clark, M. D. Segall, C. J. Pickard, P. J. Hasnip, M. J. Probert, K. Refson, and M. C. Payne, *Z. Kristallogr.* **220**, 567 (2005).
- <sup>42</sup>X. Gonze, G.-M. Rignanese, M. Verstraete, J.-M. Beuken, Y. Pouillon, R. Caracas, F. Jollet, M. Torrent, G. Zerah, M. Mikami, Ph. Ghosez, M. Veithen, J.-Y. Raty, V. Olevano, F. Bruneval, L. Reining, R. Godby, G. Onida, D. R. Hamann, and D. C. Allan, *Z. Kristallogr.* **220**, 558 (2005).
- <sup>43</sup>S. Baroni, S. de Gironcoli, A. Dal Corso, and P. Giannozzi, *Rev. Mod. Phys.* **73**, 515 (2001); X. Gonze, *Phys. Rev. B* **55**, 10337 (1997); X. Gonze and C. Lee, *ibid.* **55**, 10355 (1997).
- <sup>44</sup>S. L. Adler, *Phys. Rev.* **126**, 413 (1962); N. Wiser, *ibid.* **129**, 62 (1963).
- <sup>45</sup>F. Bruneval and X. Gonze, *Phys. Rev. B* **78**, 085125 (2008).
- <sup>46</sup>J. R. Yates, X. Wang, D. Vanderbilt, and I. Souza, *Phys. Rev. B* **75**, 195121 (2007), D. R. Hamann and D. Vanderbilt, *Phys. Rev. B* **79**, 045109 (2009).
- <sup>47</sup>X. Gonze, B. Amadon, P.-M. Anglade, J.-M. Beuken, F. Bottin, P. Boulanger, F. Bruneval, D. Caliste, R. Caracas, M. Côté, T. Deutsch, L. Genovese Ph. Ghosez, M. Giantomassi, S. Goedecker, D. R. Hamann, P. Hermetp, F. Jollet, G. Jomard, S. Leroux, M. Mancini, S. Mazevet, M. J. T. Oliveira, G. Onida, Y. Pouillon, T. Rangel, G.-M. Rignanese, D. Sangalli, R. Shaltaf, M. Torrent, M. J. Verstraete, G. Zerah, and J. W. Zwanziger, *Comput. Phys. Commun.* **180**, 2582 (2009); ABINIT is a common project of the Université Catholique de Louvain, Corning Incorporated, and other contributors.
- <sup>48</sup>R. Gomez-Abal, X. Li, M. Scheffler, and C. Ambrosch-Draxl, *Phys. Rev. Lett.* **101**, 106404 (2008).
- <sup>49</sup>M. S. Hybertsen and S. G. Louie, *Phys. Rev. B* **34**, 5390 (1986).
- <sup>50</sup>See <http://dp-code.org/> for documentation and download.
- <sup>51</sup>L. Reining, V. Olevano, A. Rubio, and G. Onida, *Phys. Rev. Lett.* **88**, 066404 (2002).
- <sup>52</sup>M. Levi, H. E. Bass, and R. R. Stern, *Handbook of Elastic Properties of Solids, Liquids, and Gases* (Academic Press, 2001), Vol. II.
- <sup>53</sup>Elastic constants were calculated by finite strain method and Vanderbilt ultrasoft pseudopotentials. In the case of diamond phases for Si and Ge, the results are:  $C_{11} = 162.8, 133.9$ ;  $C_{12} = 63.9, 49.7$ ; and  $C_{44} = 76.8, 69.1$  GPa, respectively. The average errors for the three elastic constants of the two elements are 2.66% and 2.19% for the ultrasoft and HGH pseudopotential, respectively. For Si and Ge in monoclinic phase, the elastic constants are:  $C_{11} = 147.9, 127.2$ ;  $C_{22} = 175.5, 147.1$ ;  $C_{33} = 171.1, 142.4$ ;  $C_{44} = 69, 61.9$ ;  $C_{55} = 60.4, 53.6$ ;  $C_{66} = 39, 34.2$ ;  $C_{12} = 38.5, 26.5$ ;  $C_{13} = 60.6, 44.3$ ;  $C_{15} = 12.6, 11.3$ ;  $C_{23} = 54, 42.1$ ;  $C_{25} = -6.8, -6.9$ ;  $C_{35} = 7.3, 7.1$ ; and  $C_{46} = -3.4, -2.2$  GPa, respectively. These results satisfy the stability criteria and therefore both elements are elastically stable.
- <sup>54</sup>D. R. Lide, *CRC Handbook of Chemistry and Physics*, 73rd ed. (Chemical Rubber, Boca Raton, FL, 1994).
- <sup>55</sup>H. J. McSkimin, *J. Appl. Phys.* **24**, 988 (1953).
- <sup>56</sup>R. F. S. Hearmon, *An Introduction to Applied Anisotropic Elasticity* (University Press, Oxford, 1961).
- <sup>57</sup>M. Born and K. Huang, *Dynamical Theory of Crystal Lattices* (Clarendon, Oxford, 1956).
- <sup>58</sup>Landolt-Bornstein, *Numerical Data and Functional Relationships in Science and Technology*, edited by K.-H. Hellwege, O. Madelung, M. Schulz, and H. Weiss (Springer-Verlag, New York, 1987), New Series Vol. III, p. 22a.